Quantum chaos, degeneracies, and exceptional points

W.D. Heiss and S. Radu
Centre for Nonlinear Studies and Department of Physics, University of the Witwatersrand, P.O. Wits 2050, Johannesburg, South Africa
(Received 21 April 1995)

It is argued that, if a regular Hamiltonian is perturbed by a term that produces chaos, the onset of chaos is shifted towards larger values of the perturbation parameter if the unperturbed spectrum is degenerate and the lifting of the degeneracy is of second order in this parameter. The argument is based on the behavior of the exceptional points of the full problem.

PACS number(s): 05.45.+b, 36.40.−c, 21.10.−k, 21.60.Cs

I. INTRODUCTION

The study of single-particle motion in deformed mean fields has attracted much attention recently because of its relevance to nuclear physics and for the description of metallic clusters [1,2]. For the case of harmonic oscillator potentials, deformations that go beyond a quadrupole deformation are nonintegrable and show chaotic behavior in the classical and quantum mechanical treatment. However, closer scrutiny has revealed that the addition of an octupole term to a prolate quadrupole potential produces the typical signatures of chaos only for fairly large octupole strength, in fact, the problem appears to be close to integrability. Moreover, the quantum mechanical treatment produces new shell structures for finite octupole strength even though the classical problem is nonlinear [2,3]. In contrast, the addition of an octupole term to an oblate quadrupole deformed potential yields chaos with a positive Lyapunov exponent and the corresponding quantum spectrum has the typical statistical properties ascribed to quantum chaos.

In this paper we address the question what the intrinsic properties of the quantum mechanical operators are that give rise to the different behavior described above. This question is of interest for a possible characterization of what is called quantum chaos. The example mentioned in the preceding paragraph renders a good case for such studies as it refers to the orthodox situation where a classically chaotic system is treated quantum mechanically. Our aim is to unravel the universal operator properties that produce the typical patterns ascribed to quantum chaos without reference to an underlying classical system. There was progress in previous work towards this aim as it had been recognized that, for a problem of the form $H^0 + \lambda H^1$, it is precisely the high density of the exceptional points [4,5], i.e., the singularities of the spectrum $E_n(\lambda)$, that bring about the statistical properties of the spectrum associated with quantum chaos [6]. The different aspect in the present paper is the effect of degeneracies at $\lambda = 0$ upon the behavior for $\lambda > 0$. We find that if the lifting of degeneracies is a second-order effect in λ, then the onset of chaos is suppressed and will occur only for larger values of λ. It is this pattern that explains the difference between the prolate and the oblate case as described above. The major point of the present paper is the universal validity of this finding, and the behavior of the exceptional points around $\lambda = 0$ provides for the explanation.

In the following section we introduce briefly the concept of exceptional points and present the argument for the statement made above. Section III contains examples for illustration and Sec. IV refers to the particular physical example introduced above. A summary and discussion is given in Sec. V.

II. EFFECT OF DEGENERACIES ON EXCEPTIONAL POINTS

To make the paper self-contained we briefly recapitulate the significance of exceptional points and their connection to avoided level crossings. This will facilitate the discussion about the effect of degeneracies on exceptional points and hence the global structure of the spectrum.

There is essentially a one to one relationship between avoided level crossings and exceptional points [6]. If we have a quantum mechanical problem of the form $H^0 + \lambda H^1$ with H^0 and H^1 given as $N \times N$ matrices, then the spectrum $E_n(\lambda), n = 1, \ldots, N$, is determined by one analytic function evaluated on N Riemann sheets [5]. If there are no degeneracies, the N sheets are connected by $N(N-1)$ branch points, the exceptional points. They occur in complex conjugate pairs and are the points in the complex λ plane where any two pairs of energies coalesce. If this happens sufficiently close to the real λ axis, an avoided level crossing occurs since the pair of energies coalescing in the complex plane still assumes values near each other on the neighboring real λ axis. In principle, the positions of the exceptional points are determined by the resultant of the secular equation for the spectrum, i.e., by the simultaneous solution of the two polynomial equations

$$\det(E - H^0 - \lambda H^1) = 0 \,,$$
$$\frac{d}{dE}\det(E - H^0 - \lambda H^1) = 0 \,, \tag{1}$$

which leads by elimination of E to the resultant, which

is a polynomial of order $N(N-1)$ in λ. For large values of N, an explicit calculation of the exceptional points is prohibitive. However, it is possible to determine a distribution for the real parts of the exceptional points from the knowledge of H^0 and H^1 alone [6], and in this way the regions of real λ values with large-scale avoided level crossings can be found. These are the regions where the spectrum shows the properties ascribed to quantum chaos. This method has been tested and applied to the particular physical situation of the hydrogen atom in a strong magnetic field [7].

The effect of removing degeneracies by small random perturbation was discussed previously [8]. In the present paper we address the particular problem of lifting degeneracies by the term λH^1, i.e., we assume that H^0 has certain systematic degeneracies (such as, for example, the harmonic oscillator). Guided by the particular physical problem as discussed in the Introduction and resumed in Sec. IV, we consider and compare two situations that turn out to be significantly different in the context of quantum chaotic behavior. The two situations are characterized by the presence or absence of a linear term in the expansion of $E_n(\lambda)$ in powers of λ around $\lambda = 0$.

It is obvious that the spectrum has a distinctly different behavior in the vicinity of $\lambda = 0$ for the two cases considered. A nonvanishing linear term exhibits the typical behavior of a lifting of degeneracies, when a perturbation is switched on, in that the levels fan out of the degenerate level when λ is turned on. With a zero linear term the levels stay close together and separate only when the quadratic term becomes significant. From this picture one intuitively expects that, if the additional term λH^1 produces chaos at all, the onset of chaos is delayed for increasing λ in the latter case when comparing with the former case. In the following we confirm this expectation using the exceptional points for the argument, while Sec. III presents some illustrative examples.

Each m-fold degeneracy reduces the total number of exceptional points by the number $m(m-1)$ if the linear terms are present in the expansion of the energy levels. If the leading perturbing terms are quadratic, there is a further reduction by the same number $m(m-1)$. This follows from the resultant that starts with $\lambda^{m(m-1)}$ as the lowest order in the former case and with $\lambda^{2m(m-1)}$ in the latter case. This behavior is valid for each m-fold degeneracy; in other words, if the levels have at $\lambda = 0$ the degeneracies $m_1, m_2, \ldots$, the lowest-order terms of the resultant start with $\lambda^{m_1(m_1-1)}\lambda^{m_2(m_2-1)\cdots}$ when the lifting of the degeneracy is linear and with $\lambda^{2m_1(m_1-1)}\lambda^{2m_2(m_2-1)}\ldots$ for a quadratic lifting. A particular m-fold degeneracy can be viewed as a confluent situation where $m(m-1)$ complex conjugate branch points have merged into the point $\lambda = 0$, thus canceling the singularities altogether; likewise, in the quadratic case, $2m(m-1)$ singularities have merged. The essential point of the argument lies in the comparison between the two cases: switching on linear terms leads to the emergence of $\sum_i m_i(m_i-1)$ additional exceptional points. The distance from $\lambda = 0$ of the additional exceptional points depends on the magnitude of the linear terms. For typical values they are closer to, rather than remote from, the origin. For large matrices the additional number of exceptional points can amount to many thousands. This causes avoided level crossings in the spectrum in a region where without the linear term the spectrum appears to be smooth.

III. ILLUSTRATION OF SIMPLE EXAMPLES

The realistic example that initiated this work produces more than 29 000 exceptional points for the matrix size used in our work [2]. We return to its treatment in Sec. IV. Here we illustrate the behavior of the exceptional points in a low-dimensional example. The effect on the spectrum, in particular the different onset of quantum chaos for the two different cases, is subsequently demonstrated in a generic matrix model.

We consider a nine-dimensional model where H^0 has the diagonal entries (1,1,1,2,2,2,3,3,3). The threefold degeneracies are lifted by the term λH^1 with

$$H^1(\mu) = \begin{pmatrix} \mu & 0 & 0 & 0.5 & 2 & 1.5 & 2 & 1.5 & 0 \\ 0 & 0 & 0 & 1.5 & 2 & 3 & 0.5 & 1.5 & 0.5 \\ 0 & 0 & -\mu & 2 & 3 & 1 & 2 & 1.5 & 2 \\ 0.5 & 1.5 & 2 & \mu & 0 & 0 & 1.5 & 2.5 & 0 \\ 2 & 2 & 3 & 0 & 0 & 0 & 1 & 1.5 & 1 \\ 1.5 & 3 & 1 & 0 & 0 & -\mu & 1 & 1.5 & 0.5 \\ 2 & 0.5 & 2 & 1.5 & 1 & 1 & \mu & 0 & 0 \\ 0.5 & 1.5 & 1.5 & 2.5 & 1.5 & 1.5 & 0 & 0 & 0 \\ 0 & 0.5 & 2 & 0 & 1 & 0.5 & 0 & 0 & -\mu \end{pmatrix} . \quad (2)$$

For $\mu = 0$, H^1 has only zero entries in the degenerate subspaces of H^0; therefore the nine levels of the full problem have a vanishing linear term when expanded at $\lambda = 0$. Otherwise the entries of H^1 have no significance; they have been generated randomly and any other choice (with similar orders of magnitude) yields the same qualitative result. Also, a diagonal form of H^1 in the degenerate subspaces can always be achieved by orthogonal transformations within the subspaces without changing the global spectrum. The specific form chosen is convenient as it leaves out additional irrelevant parameters and it is in line with the physical situation discussed in Sec. IV.

A nine-dimensional model yields 36 exceptional points in each half plane, our particular case reduces this num-

ber to 18. In Fig. 1(a) we display most of the exceptional points in the upper λ plane. When the parameter μ is switched on, nine additional exceptional points emerge from $\lambda = 0$ in each half plane. This is illustrated in Fig. 1(b). The basic difference between the two figures lies in the additional singularities scattered around $\lambda = 0$. Note that the other exceptional points change only moderately under variation of μ. The corresponding spectra are displayed in Fig. 2. The growing distance from the origin of the avoided crossings with increasing value μ is clearly discernible in Figs. 2(c) and 2(d), where only part of the spectrum is shown for better illustration. These avoided crossings are due to the "new" exceptional points. Note that, in particular, the levels that originate from the same degenerate energy are affected. When this occurs on a large scale, the nearest-neighbor distribution of the spectrum will typically assume the Wigner surmise for rather small values of λ while there is no resemblence to the Wigner curve when the linear terms of the perturbation vanish. This is demonstrated in the following study case.

Essentially we repeat the model used above. We consider $N > 100$ for the full dimension and the dimensions of the degenerate subspaces can be 2, 3, 4 and so on. The diagonal matrix H^0 contains the entries (1,1,...,2,2,...) and the entries of H^1 are filled randomly with elements between -1 and $+1$. The off-diagonal elements of the diagonal blocks of the degenerate subspaces are set equal to zero while the corresponding diagonals are filled with the numbers $\mu(-n_{\rm deg}/2+1/2, -n_{\rm deg}/2+1, \ldots, n_{\rm deg}/2-1/2)$ with $n_{\rm deg}$ being the dimension of the degenerate subspace. Because of the huge number of exceptional points, we no longer focus our attention on their positions. Instead, we compare nearest-neighbor distributions for $\mu = 0$ and $\mu \neq 0$ for small values of λ.

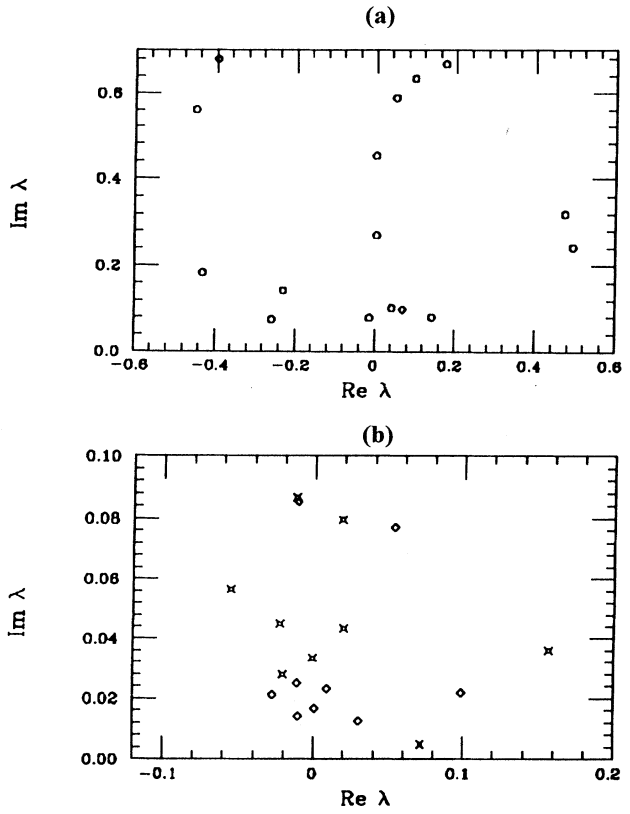

FIG. 1. Exceptional points of the nine-dimensional model in the complex λ plane for (a) $\mu = 0$ and (b) $\mu = 1/2$ (diamonds) and $\mu = 1$ (crosses). Note the difference of the scale in (a) and (b) and the motion away from the origin when μ increases.

In Fig. 3 typical results for the two different cases are presented. For the same value of λ sample averages of ten samples of nearest-neighbor distributions are illustrated for $\mu = 0$ and $\mu = 1$. There is of course a continuous transition from Fig. 3(a) to Fig. 3(b) and only if the order of magnitude of the diagonal elements of H^1 has reached that of the other matrix elements, that is, for $\mu \simeq 1$, the Wigner distribution has fully developed. We can understand, in terms of the exceptional points, why for $0 < \mu \ll 1$ the situation closely resembles that of $\mu = 0$, even though a large number of exceptional points has already emerged from the origin of the λ plane. When the exceptional points are still very close to the origin, that is, very close to each other, there is a cancellation with regard to the effect on the spectrum. In fact, two square root branch points connecting the same Riemann sheets are barely noticeable from a distance; the function $z\sqrt{z^2+\varepsilon^2}$ looks just like z^2 for $|z| \gg \varepsilon$. Only when the branch points have moved out sufficiently far does the effect on the spectrum become significant, as clearly seen in Fig. 3. The results presented refer to $n_{\rm deg} = 8$ and $N = 304$, which yields 2128 exceptional points having emerged from the origin. When $n_{\rm deg}$ is increased, the window of λ values, where this transition is strongly pronounced, becomes wider. Conversely, for smaller values of $n_{\rm deg}$ the effect is clearly seen only in a smaller range of λ values. This follows from the higher density of exceptional points associated with larger values of $n_{\rm deg}$. Also, the λ values beyond which a plain Wigner distribution occurs even when $\mu = 0$ moves closer towards the origin with increasing $n_{\rm deg}$. These two observations can qualitatively be understood from perturbative arguments in that we expect the onset of a Wigner distribution beyond the intersection point of two straight lines or parabolas from neighboring levels for $\mu \neq 0$ or $\mu = 0$, respectively; the curves intersect at $\lambda_{\rm inter}$ which is proportional to $1/n_{\rm deg}$ in the former and $1/\sqrt{n_{\rm deg}}$ in the latter case. This argument indicates where perturbation breaks down; we recall that the present paper deals with a nonperturbative situation as it is just the exceptional points that break down perturbation. We note that in a typical physical situation, such as the one discussed in Sec. IV, one is usually faced with steadily increasing values of $n_{\rm deg}$ with increasing energy.

IV. A PHYSICAL EXAMPLE

Here we present the physical example [2] that actually initiated this work. Phenomenological mean fields that contain quadrupole and octupole deformations have been investigated classically [9] and quantum mechanically [1,2] as this is of interest in nuclear physics and more

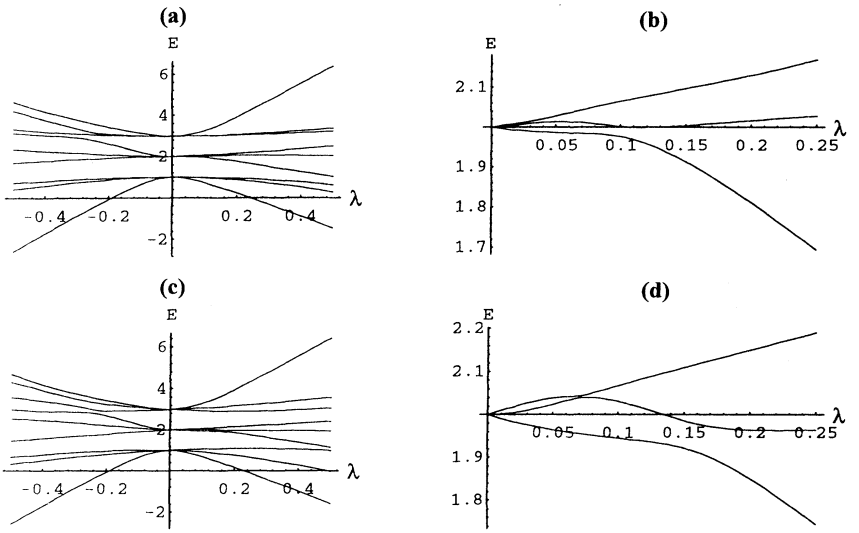

FIG. 2. Spectra of the nine-dimensional model for (a) $\mu = 0$ and (b) $\mu = 1$. For better illustration a partial view is given for (c) $\mu = 1/2$ and (d) $\mu = 1$. Note how the position of the avoided crossing not only moves outwards but also becomes more pronounced with increasing value of μ.

recently also for the description of metallic clusters. As a detailed discussion is presented in the quoted papers we here focus our attention on the aspect of interest in the present context.

The single-particle potential

$$V(\varrho, z) = \frac{m}{2}\omega^2\left(\varrho^2 + \frac{z^2}{b^2} + \lambda\frac{2z^3 - 3z\varrho^2}{\sqrt{\varrho^2 + z^2}}\right) \qquad (3)$$

describes for $b > 1$ ($b < 1$), a quadrupole deformed harmonic oscillator of prolate (oblate) shape with an additional octupole term; in fact, the term multiplying λ is proportional to $r^2 P_3(\cos\theta)$ with P_3 the third-order Legendre polynomial. We use cylindrical coordinates z and $\varrho = \sqrt{x^2 + y^2}$. For $\lambda \neq 0$ this is a two degrees of freedom system that is nonintegrable. For $b < 1$ it turns out that the switching on of the octupole term very quickly gives rise to classically chaotic behavior while the onset of chaos is barely discernable when $b \geq 2$. The statistical analyses of the correpsonding quantum spectra reveal the expected results in that for $b < 1$ the Wigner surmise is obtained for the nearest-neighbor distribution while for $b \geq 2$ a Poisson distribution is obtained and for particular values of λ even a new shell structure emerges. The latter is understood in terms of corresponding classical periodic orbits [1,2].

In the spirit of the present paper the quantum mechanical findings should be directly obtained from the matrix structure of the associated Hamiltonian and the exceptional points related to it. The appropriate basis where $H^0 = p^2/2m + m\omega^2(\varrho^2 + z^2/b^2)/2$ is diagonal is given by the occupation numbers $n_\perp$ and n_z. Note that the z component of the angular momentum is conserved and we consider here only $l_z = 0$. The arrangement of the quantum numbers in the matrix $H^1_{(n_z,n_\perp),(n'_z,n'_\perp)}$ is

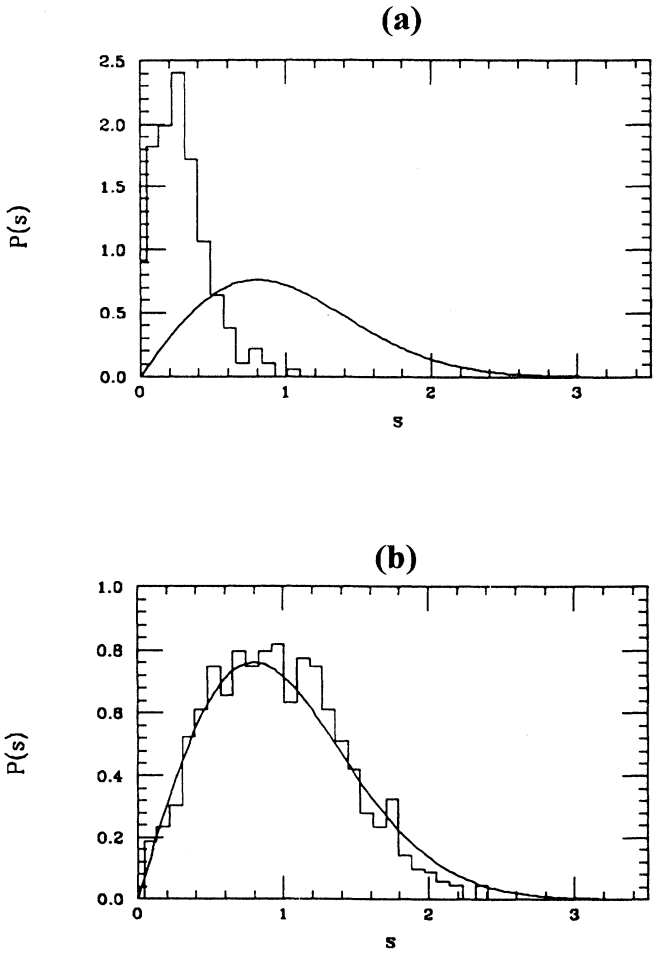

FIG. 3. Sample averages of nearest-neighbor distributions of 304 levels for (a) $\mu = 0$ with an eightfold degeneracy at $\lambda = 0$ and for (b) $\mu = 1$; both distributions are for $\lambda = 0.2$.

determined by the arithmetic ascending order of the unperturbed levels $E^0_{n_z,n_\perp}$. The arrangement will therefore depend on the value of b. The selection rules restrict entries in H^1 to $n'_z = n_z \pm (2k+1)$ and $n'_\perp = n_\perp \pm (2k)$ with $k = 0, 1, 2, \ldots$. It turns out that for $b \geq 2$ the entries vanish in the blocks of H^1, which refer to the subspaces in which the unperturbed energies E^0 are degenerate. As a consequence, the perturbative expansion at $\lambda = 0$ of the eigenvalues starts with the quadratic term. From the discussion in Sec. III it follows that a great number of exceptional points are trapped at $\lambda = 0$ and we therefore expect the onset of quantum chaos only for values of λ at an appreciable distance from zero. Using 544×544 matrices we illustrate in Fig. 4(a) the distribution of the real parts of the exceptional points for the matrix problem $H^0 + \lambda H^1$ with $b = 2$. The bulk of the exceptional points occur in fact at values of λ that fall outside the physical range (for $\lambda/\lambda_c \geq 1$ the potential no longer binds). In Fig. 4(b) we display the corresponding distribution for $b = 1/2$. Now we obtain the maximum density of exceptional points as soon as the parameter λ is switched on. This is in accordance with the results of Sec. III since now the linear term does occur in the expansion of each level around $\lambda = 0$ as there are nonzero entries in the blocks of H^1 that refer to the degenerate subspaces. The effect of this difference in the distribution of the exceptional points manifests itself in the different behavior of the respective quantum spectra in that a Wigner distribution is found for $\lambda > 0$ when $b = 1/2$, while for $b = 2$ a Wigner distribution never develops for $\lambda < \lambda_c$.

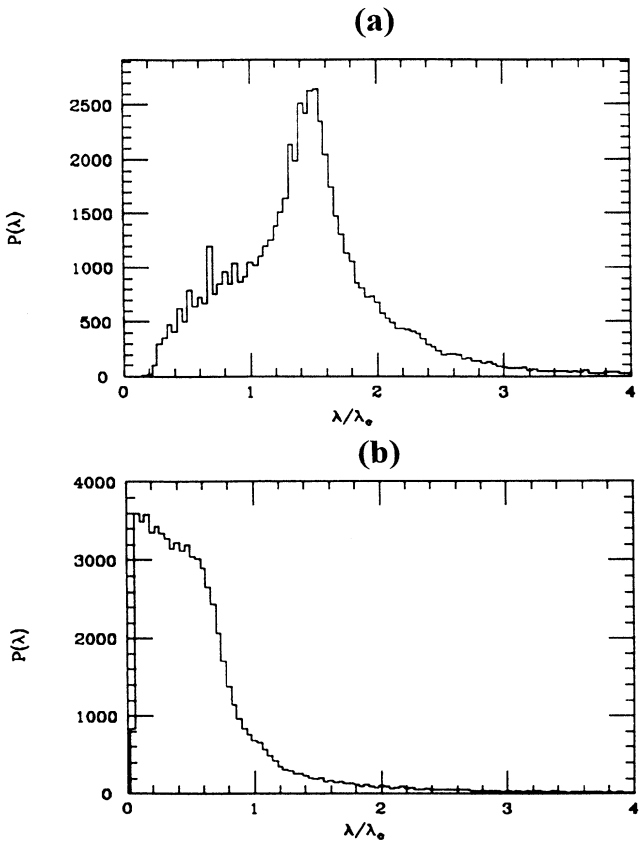

FIG. 4. Distribution of the real parts of the exceptional points for (a) the prolate case and (b) the oblate case.

V. SUMMARY AND DISCUSSION

Section IV provides a fine example where the statistical properties of the quantum spectrum can be predicted from the properties of the individual matrices H^0 and H^1 alone. To obtain the distribution of the exceptional points as illustrated in Fig. 4 it is not necessary to solve the full problem $H^0 + \lambda H^1$ let alone to determine their positions (which would be impossible for more than 295 000 exceptional points). The distribution was found using the method developed in [6,7] and explained in the Appendix. There, only some simple properties of H^0 and H^1 are used. While this result alone yields just another confirmation of the method employed in [7], the different aspect of this paper lies in the prediction that, if the unperturbed levels are degenerate to second order, level statistics ascribed to quantum chaos are substantially suppressed initially and become manifest only for sufficiently large values of the perturbation. The argument comes about rather naturally from the behavior of the exceptional points, which in turn determine the degree of quantum chaos [6]. While Sec. IV provides the physical relevance of our findings, their universal character is argued and demonstrated in Secs. II and III. To the best of our knowledge, this is the first example where even finer details with regard to level statistics can be extracted from the distribution and the general behavior of the exceptional points. We believe that more refinement can eventually even predict new shell structure as the one discovered in the model discussed. Work towards this aim is in progress.

APPENDIX: DISTRIBUTION OF THE REAL PARTS OF THE EXCEPTIONAL POINTS

We use the method of the unperturbed curves [7], where the actual spectrum is approximated by simple algebraic curves. The intesection points of the approximate curves are then identified with the real parts of the exceptional points. Since the aim is to obtain the distribution rather than the exact positions, the approximate curves suffice. They are obtained from the individual matrices H^0 and H^1 only. The requirement that the actual spectrum and the approximate curves coincide exactly for small and for large values of λ leads for the prolate case ($b = 2$) to the form

$$F_i(\lambda) = \begin{cases} \varepsilon_i + \gamma_i \lambda^2 & \text{for } \lambda \leq 0.9\lambda_c \\ (\omega_i^3 \lambda^3 + 3\omega_i^2 \alpha_i \lambda^2 + c_i \lambda + d_i)^{1/3} & \text{for} \lambda \geq 0.9\lambda_c \ , \end{cases}$$

where the ε_i and ω_i are the eigenvalues of H^0 and H^1, respectively, and

$$\gamma_i = \sum_{n \neq i} \frac{|H^1_{i,n}|^2}{\varepsilon_i - \varepsilon_n}, \quad \alpha_i = (UH^0U^{-1})_{i,i} ,$$

with U being the orthogonal matrix that diagonalizes H^1. The coefficients c_i and d_i are determined so as to smoothly match the two curves at $\lambda = 0.9\lambda_c$. We note that the second order perturbation is correct up to third order terms in λ and is in fact very close to the actual spectrum for $\lambda \leq 0.9\lambda_c$, while the expression for $\lambda \geq 0.9\lambda_c$ is correct up to terms of the order $1/\lambda$.

For the oblate case ($b = 1/2$) the spectrum is, for the purpose considered, sufficiently well approximated by the unperturbed lines

$$G_i(\lambda) = \varepsilon_i + \lambda\omega_i.$$

Recall that the eigenvalues ε_i and ω_i are different from those in the prolate case.

[1] R. Balian and C. Bloch, Ann. Phys. (N.Y.) **69**, 76 (1972); R. Arvieu, F. Brut, J. Carbonell, and J. Touchard, Phys. Rev. A **35**, 2389 (1987); W.A. Heer, Rev. Mod. Phys. **65**, 611 (1993); M. Brack, *ibid.* **65**, 677 (1993); J. Blocki, J.-J. Shi, and W.J. Swiatecki, Nucl. Phys. A **554**, 387 (1993).

[2] W.D. Heiss, R.G. Nazmitdinov, and S. Radu, Phys. Rev. Lett. **72**, 2351 (1994); Phys. Rev. B **51**, 1874 (1995); Phys. Scr. **T56**, 182 (1995).

[3] K. Arita, Prog. Theor. Phys. **90**, 747 (1993); K. Arita and K. Matsuyanagi, *ibid.* **91**, 723 (1994).

[4] C.M. Bender and T.T. Wu, Phys. Rev. D **7**, 1620 (1973); P.E. Shanley, Ann. Phys. (NY) **186**, 292 (1988); A.G. Ushveridze, J. Phys. A **21**, 955 (1988).

[5] W.D. Heiss and W.-H Steeb, J. Math. Phys. **32**, 3003 (1991).

[6] W.D. Heiss and A.L. Sannino, J. Phys. A **23**, 1167 (1990).

[7] A.A. Kotzé and W.D. Heiss, J. Phys. A **27**, 3059 (1994).

[8] W.D. Heiss and M. Müller, Phys. Rev. A **48**, 2558 (1993); W.D. Heiss and J.C.H. Chiang, *ibid.* **47**, 2533 (1993).

[9] W.D. Heiss and R.G. Nazmitdinov, Phys. Rev. Lett. **73**, 1235 (1994).